**Supplement information**

# Predict *in vitro* and *in vivo* anti-SARS-CoV-2 activity of antivirals by intracellular bioavailability and biochemical activity

**Jinwen Zhang[1,#], Mingfeng He[2,#], Qian Xie[1,3,#], Ailing Su[1], Kuangyang Yang[2], Lichu Liu[2], Jianhui Liang[1,3], Ziqi Li[1], Xiuxin Huang[4], Jianshu Hu[5], Qian Liu[1], Bing Song[1], Chun Hu[3], Lei Chen[6], Yan Wang[1]***

[1]Center for Translation Medicine Research and Development, Shenzhen Institutes of Advanced Technology, Chinese Academy of Sciences, Shenzhen 518055, China

[2]Institute of Orthopedics and Traumatology, Foshan Hospital of Traditional Chinese Medicine, Foshan 528000, China

[3]Key Laboratory of Structure-based Drug Design & Discovery (Ministry of Education), School of Pharmaceutical Engineering, Shenyang Pharmaceutical University, Shenyang 110016, China

[4]The First Clinical College of Changsha Medical College, Changsha 410219, China

[5]Department of Pharmacology, University of Oxford, OX1 3QT, UK

[6] School of Life Science and Technology, Key Laboratory of Developmental Genes and Human Disease, Southeast University, Nanjing 210096, China

[#]These authors contributed equally to this work.

***Correspondences:** Dr. Yan Wang, Center for Translation Medicine Research and Development, Shenzhen Institutes of Advanced Technology, Chinese Academy of Sciences, Shenzhen 518055, China; Tel.: +86-755-2641-7985; E-mail: yan.wang@siat.ac.cn

Jinwen Zhang current affiliation: Department of Surgery & Cancer, Faculty of Medicine, Imperial College London, South Kensington Campus, London SW7 2AZ, UK; Ailing Su current affiliation: Shanghai Institute of Materia Medica Chinese Academy of Sciences, 555 Zuchongzhi Road, Shanghai, CN 201203

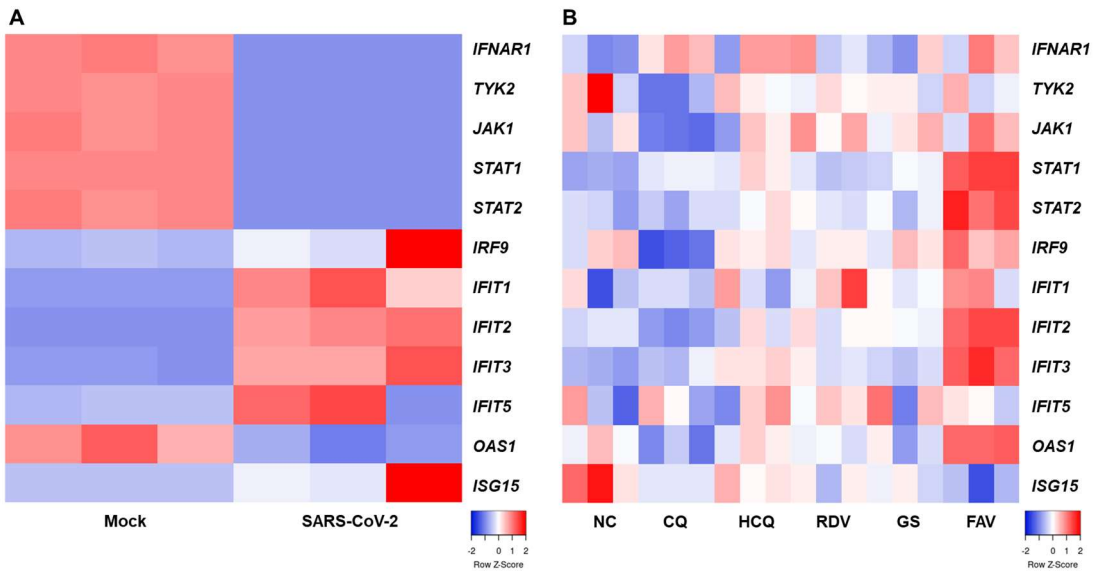


**Figure S1.** (A) SARS-CoV-2 activate IFN related genes in Vero E6 cells (n = 3 biological replicates). Data source: GSE161881. (B) Antiviral drugs did not change expression levels of IFN-activated genes compared to the vehicle controls (n = 3 biological replicates, FDR < 0.001). Cells were treated with or without antivirals at their corresponding $EC_{50}$ values for 48 h and then collected for bulk RNA sequencing. Statistical tests were embedded in DESeq2. NC: Negative control (DMSO vehicle group); CQ: chloroquine; HCQ: hydroxychloroquine; RDV: remdesivir; GS: GS-441524; FAV: favipiravir. Heatmap was generated by online service http://heatmapper.ca/.

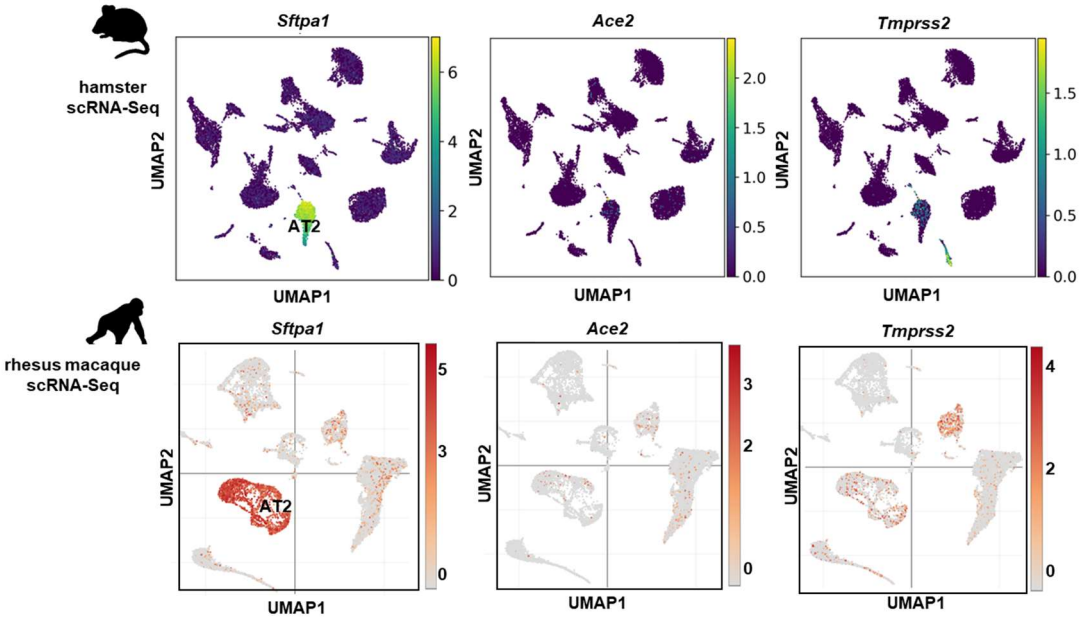


**Figure S2.** High expression of *TMPRSS2* in the AT2 cells of lung might partially explain why HCQ lost its antiviral activity *in vivo*. SARS-CoV-2 infects cells through TMPRSS2-mediated membrane fusion or cysteine protease cathepsin L (CTSL)-mediated endocytosis. The spike protein of SARS-CoV-2 is activated by the endosomal-pH-dependent CTSL. HCQ has the capability of increasing endosomal pH, therefore inhibiting CTSL-mediated endocytosis. Unlike CTSL, TMPRSS2-mediated cell entry is pH-independent, which cannot be blocked by HCQ. Therefore, high expression of TMPRSS2 can abolish antiviral activity of HCQ *in vitro*. The scRNA-seq data of hamster lung (GSE162208) were re-analyzed and visualized by Scanpy. The scRNA-seq data of rhesus macaque lung were visualized by Single Cell Portal - Broad Institute, available from https://singlecell.broadinstitute.org.

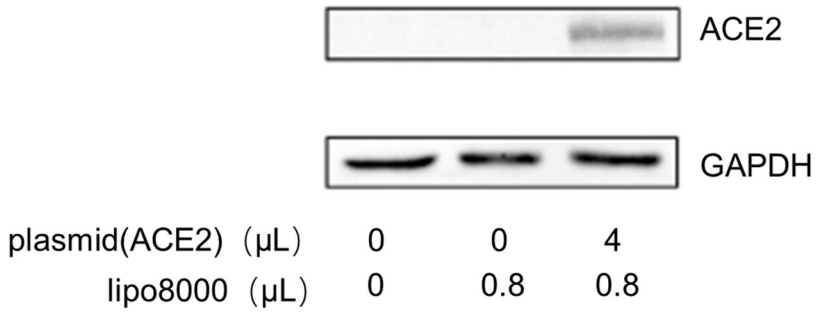


**Figure S3.** Overexpression of ACE2 in the A549 cells was confirmed by western blot. Confluent A549 cells were transfected with pcDNA3.1-ACE2-Flag plasmid (Beyotime, China) for 24 hours, and then collected for western blot.

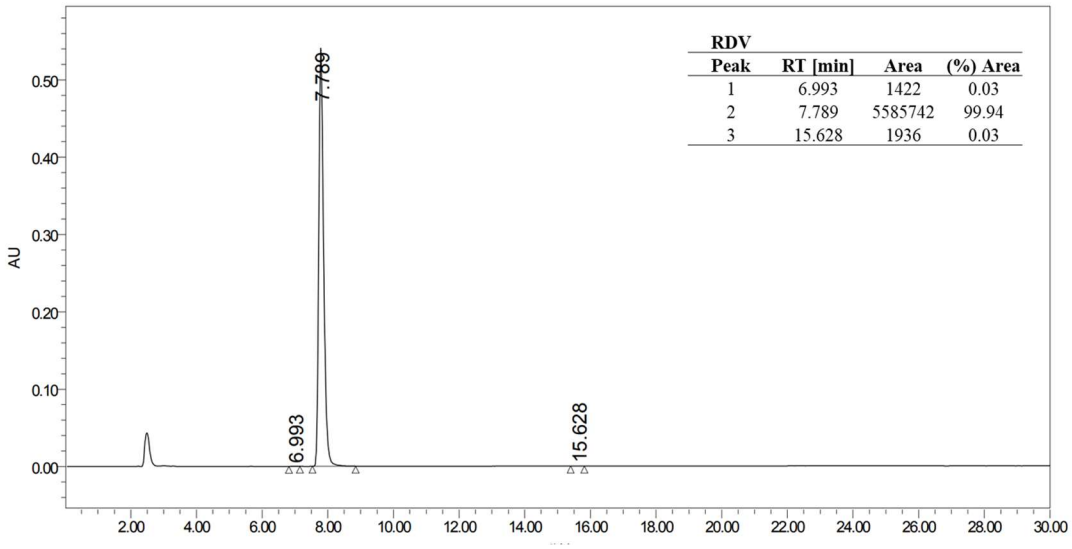


**Figure S4.** RDV quality control by analytical HPLC

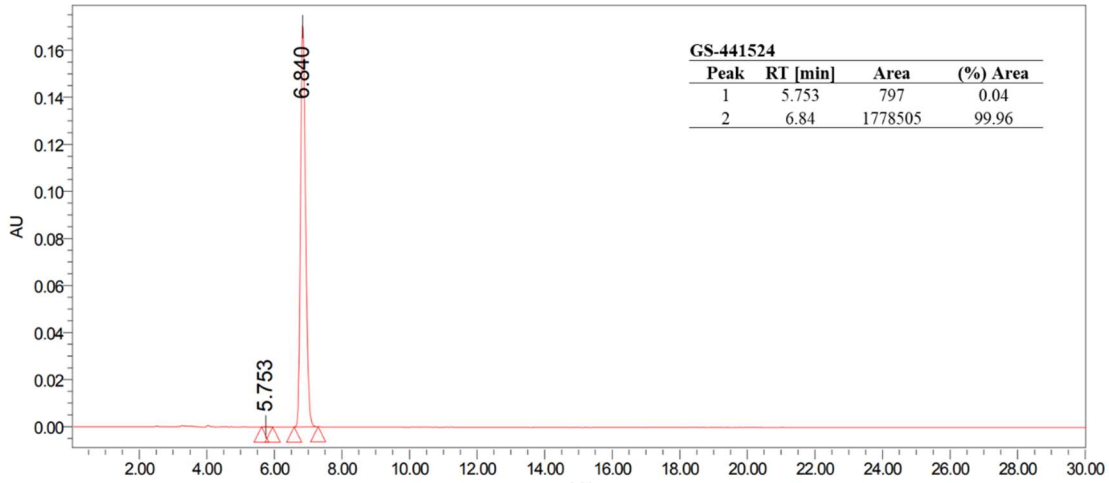


**Figure S5.** GS-441524 quality control by analytical HPLC

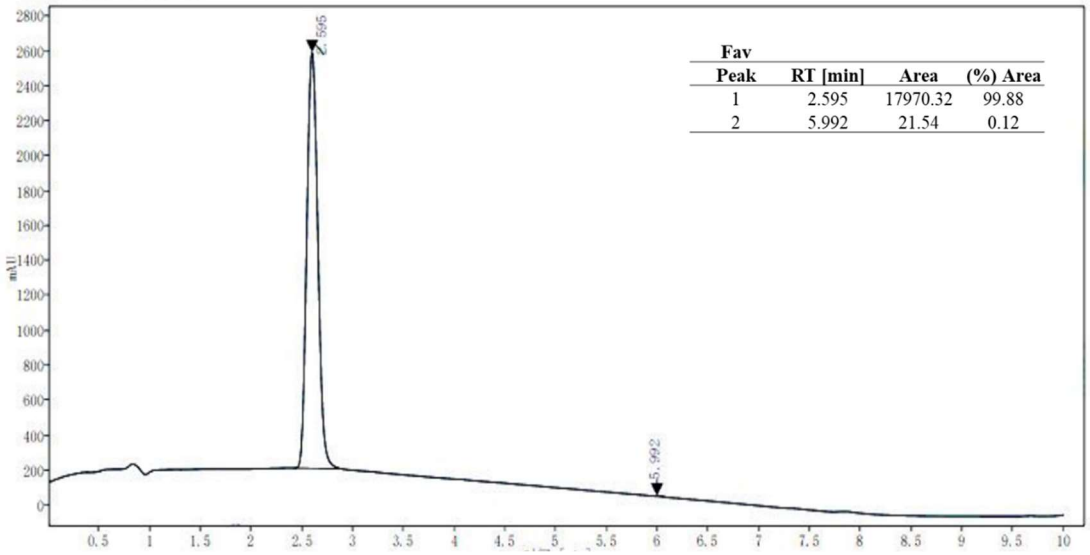


**Figure S6.** FAV quality control by analytical HPLC

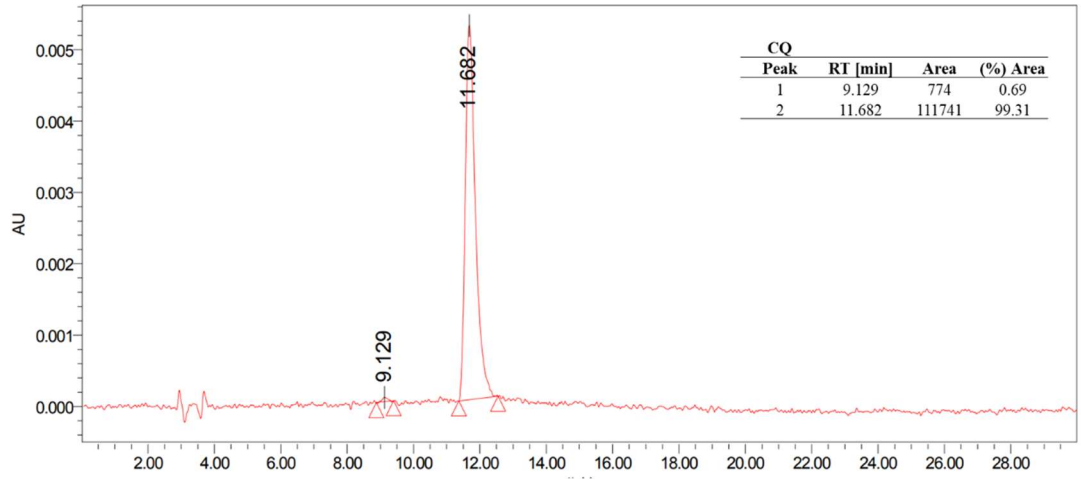


**Figure S7.** CQ quality control by analytical HPLC

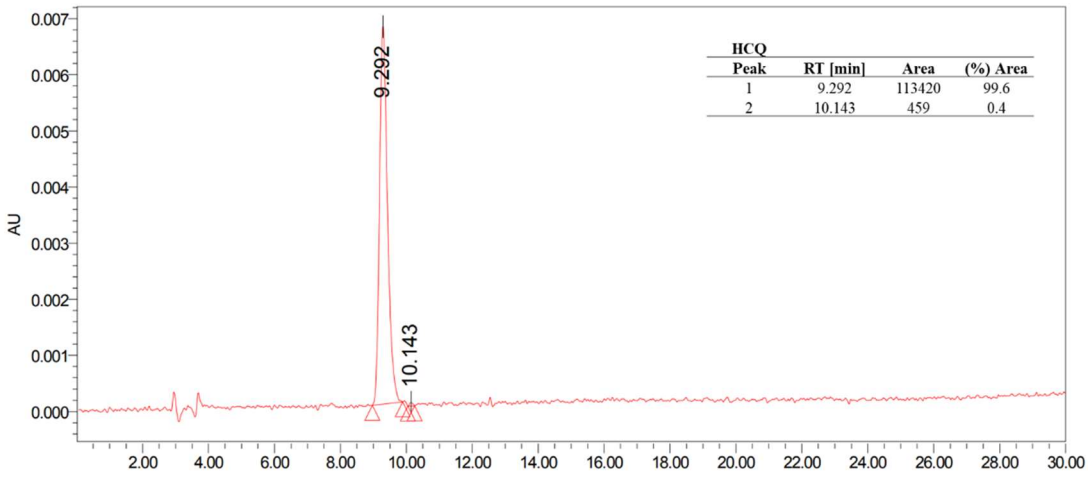


**Figure S8.** HCQ quality control by analytical HPLC

**Table S1. Comparison of the predicted $EC_{50}$ and the lung concentration of RDV**

| Verapamil-treated Vero E6 Predicted $EC_{50}$ [μM] | | |
|---|---|---|
| $K_p$ | | 20.15 |
| $F_{u,cell}$ | | 0.0014 |
| $F_{ic}$ | | 0.03 |
| Biochemical $pIC_{50}$ | | 7.49 |
| Predicted $EC_{50}$ [μM] | | 1.07 |
| Mice Lung concentration of RDV [nmol/kg] | | |
| RDV 20 mg/kg | 1h | 308 |
| | 2h | 527 |

**Table S2. Lung concentration of GS-441524**

| Treatment | GS-441524 [nmol/kg] |
|---|---|
| Mice, RDV 20 mg/kg, iv | 14237 |
| Rhesus macaque, RDV 10 mg/kg, iv | 2674 |
| Mice, GS-441524 20 mg/kg, po | 1807 |

**Table S3. Comparison of the predicted $EC_{50}$ and the lung concentration of FAV**

| Verapamil-treated Vero E6 Predicted $EC_{50}$ [μg/g] | |
|---|---|
| $K_p$ | 4.01 |
| $F_{u,cell}$ | 0.013 |
| $F_{ic}$ | 0.05 |
| Biochemical $pIC_{50}$ | 5.00 |
| Predicted $EC_{50}$ [μg/ml] | 32.00 |
| Mice Lung concentration of FAV [μg/g] | |
| FAV 6.25 mg, ip | 50.2 |
| FAV 12.5 mg, ip | 90.7 |
| FAV 25 mg, ip | 216 |

**Table S4. Comparison of the predicted EC50 and the lung concentration of HCQ/CQ**

| Verapamil-treated Vero E6 Predicted $EC_{50}$ [μM] | | |
|---|---|---|
| | HCQ | CQ |
| $K_p$ | 1956 | 2616 |
| $F_{u,cell}$ | 0.00024 | 0.00023 |
| $F_{ic}$ | 0.46944 | 0.60168 |
| Biochemical $pIC_{50}$ | 3.47 | 3.35 |
| Predicted $EC_{50}$ [μM] | 724.27 | 747.91 |
| Lung concentration of HCQ [μmol/kg] | | |
| HCQ 50 mg/kg, ip, hamster | 93 | |
| HCQ 50 mg/kg, ip, rhesus macaque | 30 | |

**Table S5. Primers used in this study**

| Primer name | | Species | Sequence(5'>3') |
|---|---|---|---|
| *GAPDH* | Forward | Human | CAGTGCCAACGTGTCAGTGGTG |
| | Reverse | Human | GTAGCCCAGGATGCCCTTGAG |
| *ABCB1* | Forward | Human | AATGGCTACATGAGAGCGGAG |
| | Reverse | Human | AATGTTCTGGCTTCCGTTGC |
| *CTSA* | Forward | Human | AAACTAGTGCCGGACAGACG |
| | Reverse | Human | GTGGTGGACGTGTTTGCTTC |
| *HINT1* | Forward | Human | TGTTCTTGGAGGTCGGCAAA |
| | Reverse | Human | AACGCAACACTCAGAGAGACT |
| *ABCC4* | Forward | Human | GGCCAAACCTCTAACCGACA |
| | Reverse | Human | TCATCCCGTTAGCAAGAGCC |
| *HPRT1* | Forward | Human | AAAGGACCCCACGAAGTGTT |
| | Reverse | Human | TACAAGAAAGTTGGGTAGGCTTTGT |
| *GAPDH* | Forward | Monkey | TCCAAAATCAAGTGGGGCGA |
| | Reverse | Monkey | AACATAGGGGCGTCAGCAG |
| *ABCB1* | Forward | Monkey | GCGAGAACATTCCTCCTCGAA |
| | Reverse | Monkey | GGCCCGGATTGACTGAATGT |
| *CTSA* | Forward | Monkey | GATCGGTGCGCGGTAGAG |
| | Reverse | Monkey | GGCTGTTCTCGGGATCCTTC |
| *HINT1* | Forward | Monkey | GGAGCTCAAGACCAGGAACTT |
| | Reverse | Monkey | CCAGGGTAGAGGCTCGAAAG |
| *ABCC4* | Forward | Monkey | GACAACTGGTATGCCTTGCC |
| | Reverse | Monkey | CCACATTTGCCGTTGCTTCA |
| *HPRT1* | Forward | Monkey | CCTGCTTCTCCTCAGCTT |
| | Reverse | Monkey | TCACTAATCACGACGCCAGG |

**Table S6. Final concentrations of different drugs in the accumulation assay**

| Drug name | Concentration (μM) |
|---|---|
| chloroquine | 20 |
| hydroxychloroquine | 20 |
| favipiravir | 65 |
| remdesivir | 10 |
| GS-441524 | 10 |

**Table S7. Chromatographic and Mass condition of RDV and GS-441524**

| Chromatographic condition | | | |
|---|---|---|---|
| | Time (min) | Mobile phase A (%) | Mobile phase B (%) |
| remdesivir | 0 | 95 | 5 |
| | 1 | 10 | 90 |
| | 2.8 | 10 | 90 |
| | 3 | 95 | 5 |
| | 6 | 95 | 5 |
| GS-441524 | 0 | 97 | 3 |
| | 1.5 | 20 | 80 |
| | 2.8 | 20 | 80 |
| | 3 | 97 | 3 |
| | 6.5 | 97 | 3 |
| MS condition | | | |
| | Precursor ion (m/z) | Product ion (m/z) | Collision energy (eV) |
| remdesivir | 603 | 402 | 22 |
| GS-441524 | 292 | 202 | 22 |

**Table S8. Specific concentration to make D=100**

| Cell line | D | Cell volume (μL) | Concentration (cells/ml) |
|---|---|---|---|
| A549 | 100 | 9.05E-07 | 1105275 |
| Vero E6 | 100 | 2.57E-06 | 388747 |
| Calu-3 | 100 | 4.19E-06 | 238739 |